Environmental and Experimental Botany 131 (2016) 77–88

Contents lists available at ScienceDirect

Environmental and Experimental Botany

journal homepage: www.elsevier.com/locate/envexpbot

Impact of magnetite iron oxide nanoparticles on wheat (*Triticum aestivum* L.) development: Evaluation of oxidative damage

María Florencia Iannone[a,*], María Daniela Groppa[a], María Elisa de Sousa[b], Marcela Beatriz Fernández van Raap[b], María Patricia Benavides[a]

[a] *Instituto de Química y Fisicoquímica Biológicas (IQUIFIB-CONICET), Departamento de Química Biológica, Facultad de Farmacia y Bioquímica, Universidad de Buenos Aires, Junín 956, 1113 Buenos Aires, Argentina*
[b] *Instituto de Física de La Plata (IFLP- CONICET), Departamento de Física, Facultad de Ciencias Exactas, Universidad Nacional de La Plata, c.c. 67, 1900 La Plata, Argentina*

ARTICLE INFO

Article history:
Received 14 April 2016
Received in revised form 12 July 2016
Accepted 13 July 2016
Available online 15 July 2016

Keywords:
Fe_3O_4
Magnetite
Nanoparticles
Oxidative damage
Triticum aestivum L.
Wheat

ABSTRACT

Interest on the environmental impact of engineered nanomaterials has rapidly increased over the past years because it is expected that these materials will eventually be released into the environment. In this work, physiological effects and possible cell internalization of citric acid coated-Fe_3O_4 nanoparticles (5, 10, 15, 20 mg L^{-1}) on wheat (*Triticum aestivum* L.) plants grown five days under hydroponic conditions were evaluated. Visualization of root sections by transmission electron microscopy showed that Fe_3O_4 nanoparticles entered the root through the apoplastic route and were then detected in the root epidermal cell walls. Moreover, strong magnetic signals detected by vibrating sample magnetometry (VSM) and a huge increment in the Fe content (8,07 and 2,01 mg g^{-1} DW for NP20 and C-NP20 treatments respectively) were observed in wheat roots treated with Fe_3O_4 nanoparticles. However, no superparamagnetic signal was detected in the aerial part which indicated that magnetite nanoparticles were not translocated by vascular tissues in wheat plants in the experimental conditions of this study.

Moreover, Fe_3O_4 nanoparticles did not affect the germination rate, the chlorophyll content, and the plant growth, and they did not produce lipid peroxidation, nor alter $O_2^{\bullet-}$ or H_2O_2 accumulation respect to control plants. Furthermore, electrolyte release and cell death percentage were not modified by nanoparticle treatment. The antioxidant enzyme activities of NP treated plants significantly increased in both the root and the aerial part respect to the controls, showing a response leading to prevent oxidative damage. These preliminary results show that these Fe_3O_4 nanoparticles are not phytotoxic, suggesting that they could potentially be useful for the design of new products for agricultural use.

1. Introduction

The proliferation and release into the environment of engineered 1–100 nm diameter nanoparticles (NPs) worldwide raise important ecological and human health concerns. The increasing use of different nanoparticles for biological and industrial purposes has made necessary to go deep into the knowledge about the potential adverse effects of these nanomaterials on living organisms, since they could be transported by water and accumulate in soils (Ma et al., 2015; Hossain et al., 2015).

Considering that food materials are not only a source of nutrients but also contribute to the health of consumers, and that plants may transport NPs into the food chain, NPs could be a threat to humans and animals.

There are many reports concerning NPs uptake, translocation and toxicity in plants, but the published results are somewhat contradictory, showing variations depending on the NPs used, their size and the plant species (Arruda et al., 2015; Chichiriccò and Poma, 2015; Lin and Xing, 2007; Ma et al., 2015; Miralles et al., 2012; Ren et al., 2011 and references therein).

The first study using Fe_3O_4 NPs in plants was made by Zhu et al. (2008), who demonstrated a significant uptake of these types of NPs by pumpkin plants and their subsequent translocation and accumulation in various tissues. In soybean plants, it has been reported that iron oxide NPs affected chlorophyll content and might have influence on both biochemical and enzymatic

Abbreviations: CA, citric acid; DW, dry weight; FW, fresh weight; NPs, nanoparticles; TEM, transmission electron microscopy; VSM, vibrating sample magnetometry.

* Corresponding author.
E-mail address: mfiannone@ffyb.uba.ar (M.F. Iannone).

http://dx.doi.org/10.1016/j.envexpbot.2016.07.004
0098-8472/

efficiency in different stages of the photosynthesis reactions (Ghafariyan et al., 2013).

Although most NPs have a greater size than plant cell wall pores (3.5–5 nm) (Chichiriccò and Poma, 2015; and reference therein), it has been shown they can enter plant root cells through different mechanisms, including aquaporins (Miwa et al., 2010), endocytosis (Eggenberger et al., 2009), membrane transport systems (Miwa et al., 2010; reviewed by Gojon et al., 2009), by binding to carrier proteins or organic chemicals in the environmental media (Rico et al., 2011), creating new pores by crosslinking of components of the cell wall (Fleischer et al., 1999). According to the type of NPs, they can be accumulated in roots or be translocated to other tissues *via* xylem and phloem (Cifuentes et al., 2010). The movement of NPs between cells could occur through plasmodesmata and, inside the cells, they can be transported by endo-exocytosis or *via* apoplast and symplast (Chichiriccò and Poma, 2015; Cifuentes et al., 2010; and reference therein; Rico et al., 2011). It has been proposed that vascular tissues might play a significant role in the long-distance bulk transport of NPs (Ma et al., 2010), as occurred with CuO nanoparticles, that were transported upward by xylem and downward by phloem in maize plants (Wang et al., 2012). However, further studies are needed to understand the exact mechanisms of uptake, transport and impact of different NPs in several plant species.

Iron oxide magnetite NPs, which are generally considered to be biologically and chemically inert (Ren et al., 2011), are useful for imaging and separation techniques due to their magnetic properties. Besides, these NPs can be coated with catalysts or enzymes in order to obtain NPs with a dual function: separation and detection (Gao et al., 2007). Moreover, Fe_3O_4 NPs are increasingly used in the biomedical field (Kohler et al., 2005; Mahmoudi et al., 2011) and for environmental remediation (Liu et al., 2008; Shipley et al., 2011; Yantasee et al., 2007). In this context, the objective of this work was to determine if Fe_3O_4 NPs had toxic effects on germination and the early stages of growth of wheat plants in order to discard potential toxic effects at this essential stage, considering that these nanomaterials could be promisingly used as inoculant carriers. Taking into account that future inoculants could be formulated based on a NP concentration that did not inhibit the bacterial growth, in this work we decided to work with NP concentrations up to 20 mg L^{-1}, as has been reported by other authors that used Fe_3O_4 NPs in bacteria (Ghalamboran et al., 2009; Ghalamboran and Ramsden, 2010).

2. Materials and methods

2.1. Nanoparticles synthesis and properties

Fe_3O_4 nanoparticles were prepared by co-precipitation of ferric chloride and ferrous chloride in the presence of excess ammonia NH_4OH solution as described in de Sousa et al. (2013). The obtained magnetite cores were negatively charged by citric acid (CA) adsorption over its surfaces. Magnetite nanoparticles ~10 nm size, electrostatically stabilized by CA coating (Z-potential = −36 mV), with hydrodynamic sizes in the range~18 nm and well dispersed in aqueous solution were obtained. The electrostatic stabilization prevented aggregation during the uptake time, assuring that seeds or roots were in contact with the NPs in the whole volume of treatment solution. A colloid concentration of 20 mg ml^{-1} NPs (expressed as Fe_3O_4 mass per solution volume) was determinated within an accuracy of 2% using $K_2Cr_2O_7$ as titrant agent.

2.2. Stability assays of nanoparticles

Magnetite nanoparticles or equal millilitres of nanoparticles and Hoagland solution were electrophoresed on 2.5% horizontal agarose gel at 80 V applied voltage in order to evaluate surface charge, electrophoretic mobility and the level of purity (Morneau et al., 1999; Sahoo et al., 2005).

A turbidimetric method was used to deduce the stability in the Hoagland solution. Absorbance as a function of time was measured at 700 nm in a Hitachi U-2000 spectrophotometer (Zins et al., 1999).

2.3. Plant growth conditions and treatments

Wheat (*Triticum aestivum* L.) seeds (provided by Nidera, Argentina) were germinated on Petri dishes containing 10 ml of the treatment solution (distilled water, 5, 10, 15 or 20 mg L^{-1} of magnetite NPs in distilled water) and then placed in an incubator in the dark at 24 °C over a period of 48 h. After this time, seedlings were transferred to a hydroponic system with Hoagland (Hoagland and Arnon, 1950) solution (C) or Hoagland solution containing the NPs concentrations mentioned above. Thus, the treatments were called NP5, NP10, NP15 and NP20. When seeds were germinated in distilled water and then exposed to the NPs treatments in the hydroponic system, the treatments were called C followed by NPs concentration (C-NP): C (Hoagland solution) C-NP5, C-NP10, C-NP15 and C-NP20.

Treatment solutions were replaced daily. Plants were grown with a 16/8 h photoperiod at 26/20 °C, under fluorescent white light (photon flux density: 175 μmol m^2 s^{-1}) in a controlled environmental growth chamber. They were harvested after five days of growth and roots and aerial parts were used for analysis.

2.4. Evaluation of magnetite toxicity on wheat seed germination and seedlings growth

The germination rate of wheat seeds was recorded after the emergence of the radicle during the first 48 h of growth in distilled water or NPs treatment solutions.

To investigate the toxicity of magnetite NPs on seedling growth, a pool of 25–30 plants per treatment (C, NP or C-NP) was used to measure root or aerial part length after five days of growth on each treatment solution.

2.5. Chlorophyll content

For chlorophyll determination, 100 mg FW of wheat leaves were incubated in 5 ml of 96% ethanol at 50–60 °C until complete bleaching. Chlorophyll content was then measured spectrophotometrically at 654 nm on the ethanolic supernatant in a Hitachi U-2000 spectrophotometer, as described by Wintermans and de Mots (1965).

2.6. Iron determination

To analyze the metal concentration, seeds, roots or aerial parts were dried during 15 d at 80 °C and ground. The fine powder obtained (about 100 mg DW) was digested in a mixture of HNO_3: $HClO_4$ (3:1 v/v) at 170 °C and the metal determination was performed by flame atomic absorbance spectrometry (Perkin Elmer Analyst 300).

2.7. Oxidative stress

2.7.1. In situ $O_2^{\bullet-}$ localization

$O_2^{\bullet-}$ content was estimated using a 0.05% (w/v) solution of nitroblue tetrazolium (NBT), which reacts with $O_2^{\bullet-}$ and produces a blue precipitate of formazan. DPI (a NADPH oxidase inhibitor) was used as a control (Bolwell et al., 1998; Frahry and Schopfer, 1998).

2.7.2. In situ H_2O_2 *localization*

H_2O_2 formation was determined by an histochemical method using 3,3′ diaminobenzidine (DAB). The appearance of brown spots is indicative of H_2O_2 formation (Thordal-Christensen et al., 1997). Ascorbic acid (an antioxidant) was used as a control.

2.7.3. Thiobarbituric acid reactive substances (TBARS) determination

The level of lipid peroxidation products in roots and aerial parts were determined by estimating thiobarbituric acid reactive substances (TBARS) as described by Heath and Packer (1968). TBARS content was calculated using the extinction coefficient (155 mM^{-1} cm^{-1}).

2.7.4. Enzyme preparations and assays

Plant homogenates for determination of ascorbate peroxidase (APOX, EC 1.11.1.11), guaiacol peroxidase (GPOX, EC 1.11.1.7), superoxide dismutase (SOD, EC 1.15.1.1) and catalase (CAT, EC 1.11.1.6) were prepared in 50 mM phosphate buffer pH 7.8 containing 0.5 mM EDTA, 1 g PVP, and 0.5% (v/v) Triton X-100. APOX activity was immediately determined in the supernatant according to Nakano and Asada (1981). GPOX activity was determined as described by Maehly and Chance (1954), SOD activity was assayed as described by Becana et al. (1986) and CAT activity was determined according to Chance et al. (1979).

2.8. Cell death detection and membrane damage

2.8.1. Evans blue staining

To determine changes in cells viability upon exposure to magnetite nanoparticles, wheat leaves were incubated with a 0.25% (w/v) aqueous solution of Evans Blue (Baker and Mock, 1994) during 15 min at room temperature, then washed twice with distilled water and left in distilled water overnight. Then the samples were incubated 1 h at 50 °C with a methanol-SDS solution and the absorbance was measured at 595 nm.

2.8.2. Electrolyte leakage

For electrolyte leakage measurement, root and aerial part samples were thoroughly washed with distilled water and kept in closed vials with 10 ml of deionized water. To estimate ion leakage (Shou et al., 2004), conductivity of each solution was measured at the initial time (To), after the incubation with the different treatments (T1) and after heating at 100 °C for 1 h (T2). The results were expressed as relative conductivity $[(T1 - T0)/(T2 - T0)] \times 100$.

2.9. Magnetization measurement

Another set of dried roots, seeds and aerial parts from C, C-NP or NP treatments were used to detect the presence of NPs and to estimate the NPs uptake. The specific magnetization (M) was measured as a function of the applied magnetic field (H) at room temperature. The magnetization measurements were performed in duplicate.

Magnetization measurements were carried out at room temperature using a vibrating sample magnetometry (VSM) LakeShore 7404 with maximum field of 20,000 Oe (Wang et al., 2011).

2.10. Transmission electron microscopy analysis

Segments (1 mm diameter, 10 mm length) were taken from the seedling roots including the root tip, and from shoots. To visualize the NPs uptake, some samples were fixed and observed using transmission electron microscopy (TEM). Wheat samples (roots or shoots) were prefixed in 2% glutaraldehyde, washed in 0.1 mol L^{-1} pH 7 phosphate buffer with sucrose, postfixed in 1.5% (w/v) osmium tetroxide, dehydrated in acetone, and infiltrated and embedded in epoxy resin (Lin and Xing, 2008). Thin sections were cut from the embedded samples using an ultramicrotome equipped with a diamond knife. The sections were examined by transmission electron microscopy without contrasting (TEM Zeiss 109 T with GATAN digital camera).

2.11. Statistics

All data presented are the mean values of three independent set of experiments. Each value was presented as means ± standard errors (SE), with a minimum of three replicates. Statistical analysis was carried out by one-way ANOVA using the Tukey test to

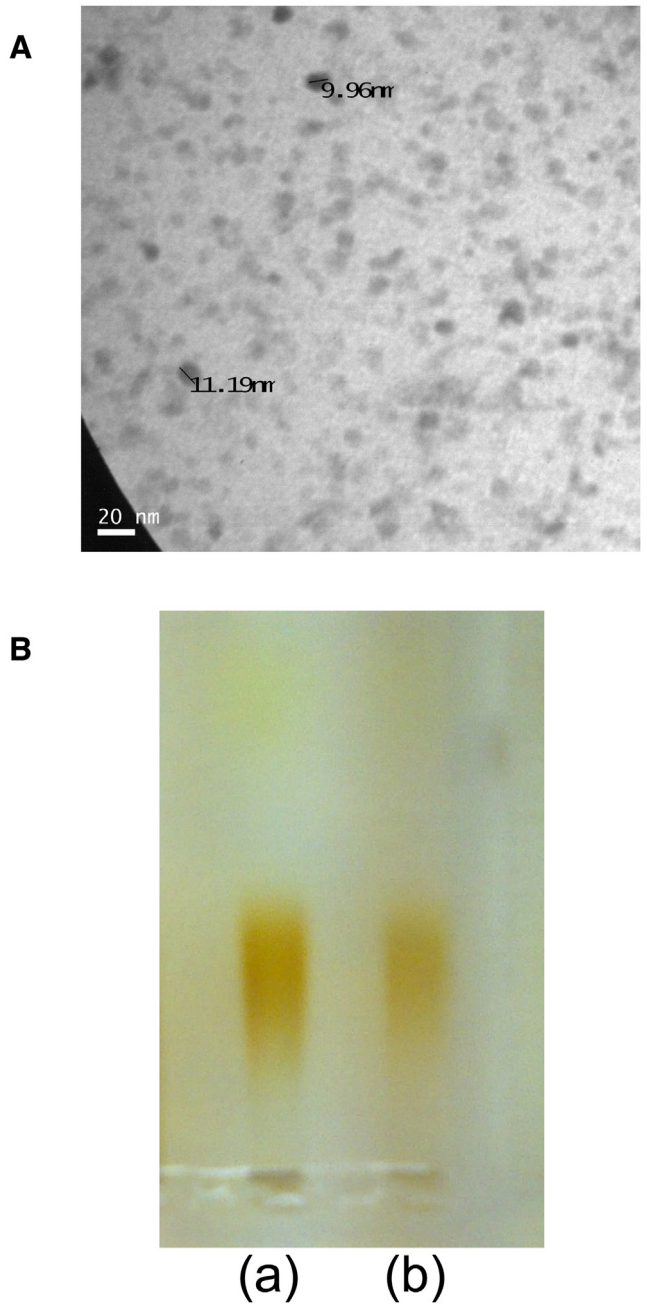

Fig. 1. (A) Transmission-electron microscopy (TEM) images of Fe_3O_4 nanoparticles. (B) Electrophoresis of citric acid coated magnetic particles (a) in distilled water, (b) in Hoagland solution.

evaluate whether the means were significantly different, taking one asterisk $^{*}p < 0.05$, two asterisks $^{**}p < 0.01$, and three asterisks $^{***}p < 0.001$ as significant.

3. Results

3.1. Fe_3O_4 nanoparticles analysis

Fig. 1A shows a typical TEM image of CA-coated magnetite nanoparticles in water suspension. The mean size of Fe_3O_4 nanoparticles was 10.9 ± 1.8 nm (n = 25).

An electrophoretic assay was performed to determine if the surface charge of NPs was affected by the Hoagland solution. Fig. 1B shows that Fe_3O_4 NPs were stable in the nutrient solution as they migrated to the same distance from the origin. At the same time, Fe_3O_4 NPs in water or in Hoagland solution have no changes in absorbance as a function of time (data not shown), indicating that the NPs suspension was not aggregated.

3.2. Effect of Fe_3O_4 NP treatment on seed germination, chlorophyll content and plant elongation

The Fe_3O_4 NP localization was studied at germination and during the first 5 days of growth of wheat plants. Seed germination was not affected by Fe_3O_4 NP treatment (Fig. 2A). The averaged seed germination rate for all treatments was 90%. As can be seen from Fig. 2B and C, chlorophyll content was similar in all wheat leaves, independently of the treatment and the moment of the application of treatments.

Wheat aerial part length of plants treated with Fe_3O_4 NPs from the start of germination (NP treatment) was not significantly different from that of the control ($p \geq 0.05$, Fig. 3A), but the root

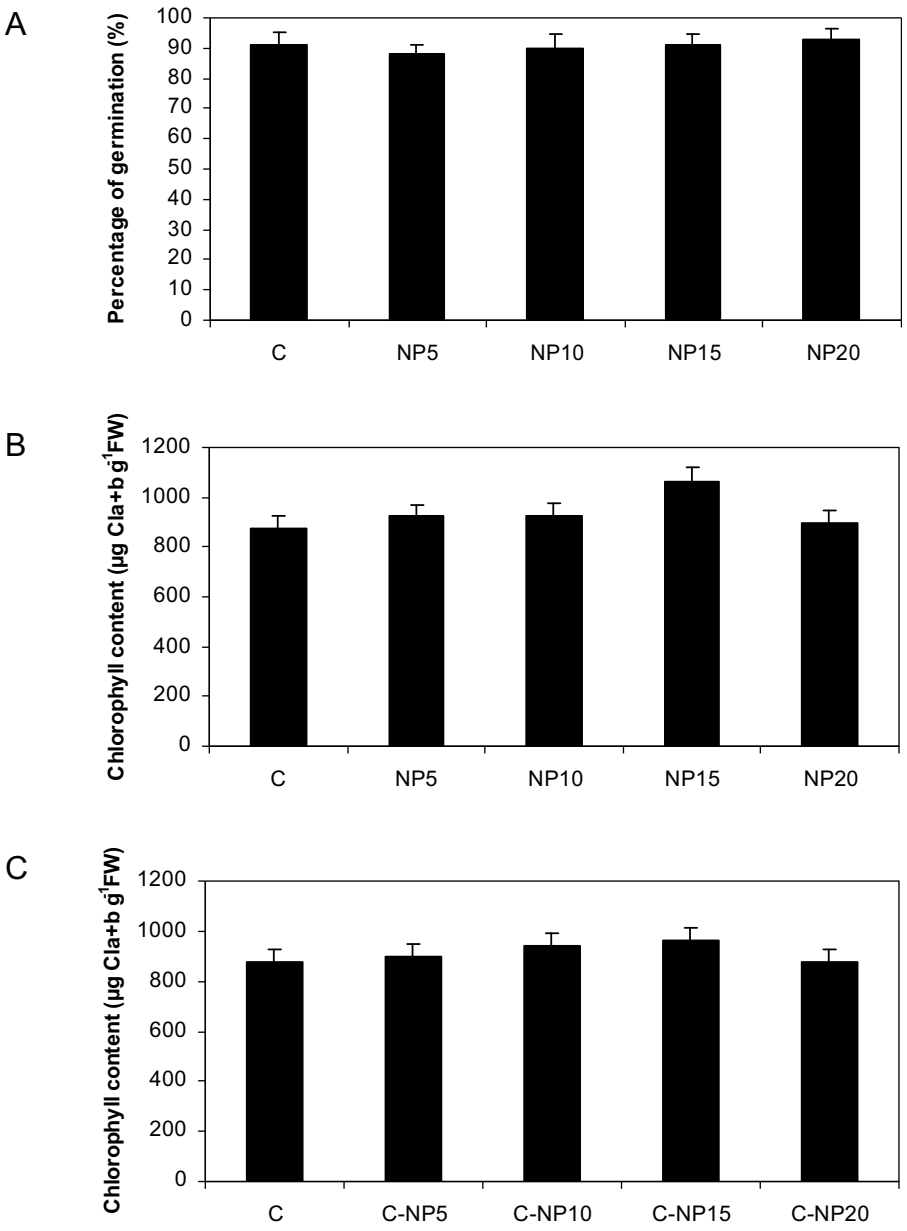

Fig. 2. (A) Percentage of germination of *Triticum aestivum* L. seeds treated with 5 (NP5), 10 (NP10), 15 (NP15), 20 (NP20) mg L^{-1} Fe_3O_4 nanoparticles. (B) Chlorophyll content in wheat plants exposed to 5 (NP5), 10 (NP10), 15 (NP15), 20 (NP20) mg L^{-1} Fe_3O_4 nanoparticles from germination. (C) Chlorophyll content in wheat plants exposed to 5 (C-NP5), 10 (C-NP10), 15 (C-NP15), 20 (C-NP20) mg L^{-1} Fe_3O_4 nanoparticles after germination. Values are the mean ± SE of three different experiments with five replicated measurements.

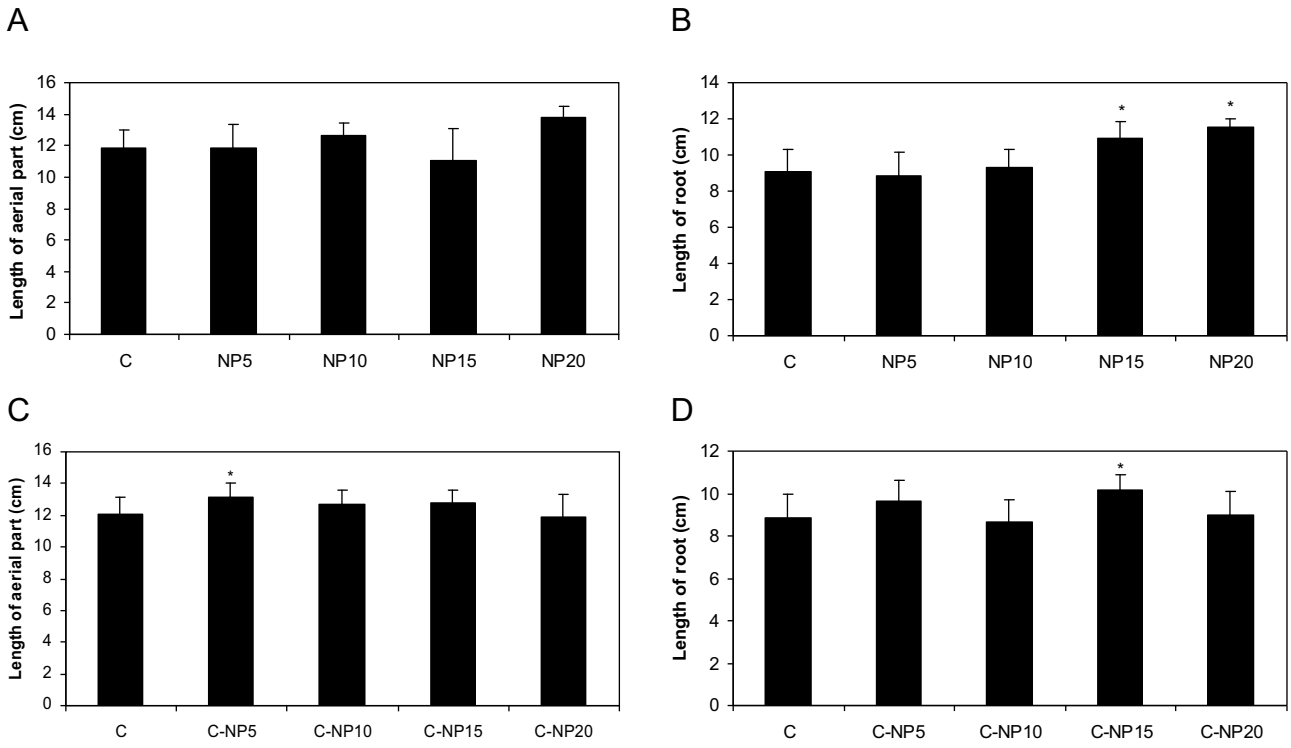

Fig. 3. Effect of Fe_3O_4 nanoparticles on wheat (*Triticum aestivum* L.) growth. Plants exposed to 5 (NP5), 10 (NP10), 15 (NP15), 20 (NP20) mg L^{-1} Fe_3O_4 nanoparticles from germination: (A) Length of aerial part (B) Length of roots. Plants exposed to 5 (C-NP5), 10 (C-NP10), 15 (C-NP15), 20 (C-NP20) mg L^{-1} Fe_3O_4 nanoparticles after germination: (C) Aerial part length (D) Root length. Values are the mean ± SE of three different experiments with six replicated measurements. Asterisks indicate significant differences (*, $p < 0.05$) according to Tukey's multiple range test.

length increased 20% with 15 and 20 mg L^{-1} of NPs (Fig. 3B, NP15 and NP20, $p < 0.05$). When wheat plants were treated with NPs after germination (C-NP treatment) the root length increased only with 15 mg L^{-1} of NPs (Fig. 3D, C-NP15, $p < 0.05$) and the aerial part length with 5 mg L^{-1} of NPs (Fig. 3C, C-NP5 $p < 0.05$).

3.3. Total iron content

Total iron content of plant roots, aerial parts and seeds are shown in Table 1. The total Fe content in seeds or in the aerial part was not significantly different among treatments. However, the total Fe content in roots of NP20 treatment was twenty times higher than the control, while plants exposed to magnetite NPs just in the hydroponic system (C-NP20) quintupled the Fe content of control roots.

3.4. Magnetization in plants

Fig. 4A shows the superparamagnetic behaviour of CA-Fe_3O_4 colloid. Selected VSM measurement results from wheat root tissues treated with 20 mg L^{-1} of CA-Fe_3O_4 NPs from germination (NP20) or after germination (C-NP20) are illustrated in Fig. 4B together with control sample measurement (C). The control sample displayed a diamagnetic behaviour (straight line) characteristic of organic material, while NP20 and C-NP20 showed a typical superparamagnetic behaviour similar to the one recorded for CA- Fe_3O_4 colloid (see Fig. 4A). From the fit with a Langevin model of the data in Fig. 4A a saturation magnetization of 15 emu g^{-1} DW Fe_3O_4 was inferred. The saturation magnetization of NP20 and C-NP20 are two orders of magnitude lower than CA-Fe_3O_4 colloid. The uptake amount as obtained from VSM data is 3 and 10 mg Fe g^{-1} DW in root for C-NP20 and NP20 treatments, respectively. These values are in good agreement with flame atomic absorbance spectrometry listed in Table 1.

Fig. 4C shows field dependence magnetization of C, C-NP20 and NP20 of aerial part tissues and of C and NP20 of seeds. The behaviour is predominantly diamagnetic for all this samples, but C, C-NP20 and NP20 of aerial part display a weak ferromagnetic signal, with a magnetization three orders of magnitude lower than C-NP20 or NP20 root treatment. This signal, clearly shown in the inset where the central part of the M *vs.* H data was amplified for these samples, may be related to Fe incorporated to the apoferritin from the Fe-EDTA of the Hoagland solution. Neither ferromagnetic signal was detected nor in the empty sample holder nor in the Hoagland solution.

These results suggest that Fe_3O_4 NPs were not transported from the root to the aerial part under the studied conditions despite they were absorbed from the solution. However, a significant magnetization with the Fe_3O_4 NP treatments was observed in the roots samples. In plants exposed to 20 mg L^{-1} Fe_3O_4 NPs from germination (NP20), the magnetization in roots was 0.205 emu g^{-1}, and in plants treated after germination (C-NP20) was 0.0620 emu g^{-1}, indicating that a higher amount of iron was accumulated in roots

Table 1
Total Fe content in seeds, roots and aerial parts of wheat plants (*Triticum aestivum* L.) treated with 20 mg L^{-1} Fe_3O_4 nanoparticles.

Iron content (mg g^{-1}DW)	C	NP20	C-NP20
Seed	0.22 ± 0.01	0.21 ± 0.01	0.22 ± 0.01
Root	0.41 ± 0.01	8.07 ± 0.04***	2.01 ± 0.03***
Aerial part	0.32 ± 0.01	0.35 ± 0.02	0.34 ± 0.00

C, NP20, C-NP20 mean control plants, plants treated with 20 mg L^{-1} Fe_3O_4 nanoparticles from germination or after germination, respectively. Data are the mean ± SE of three independent experiments, with five replicates for each treatment. Asterisks within rows indicate significant differences (***$p < 0.001$), according to Tukey's multiple-range test.

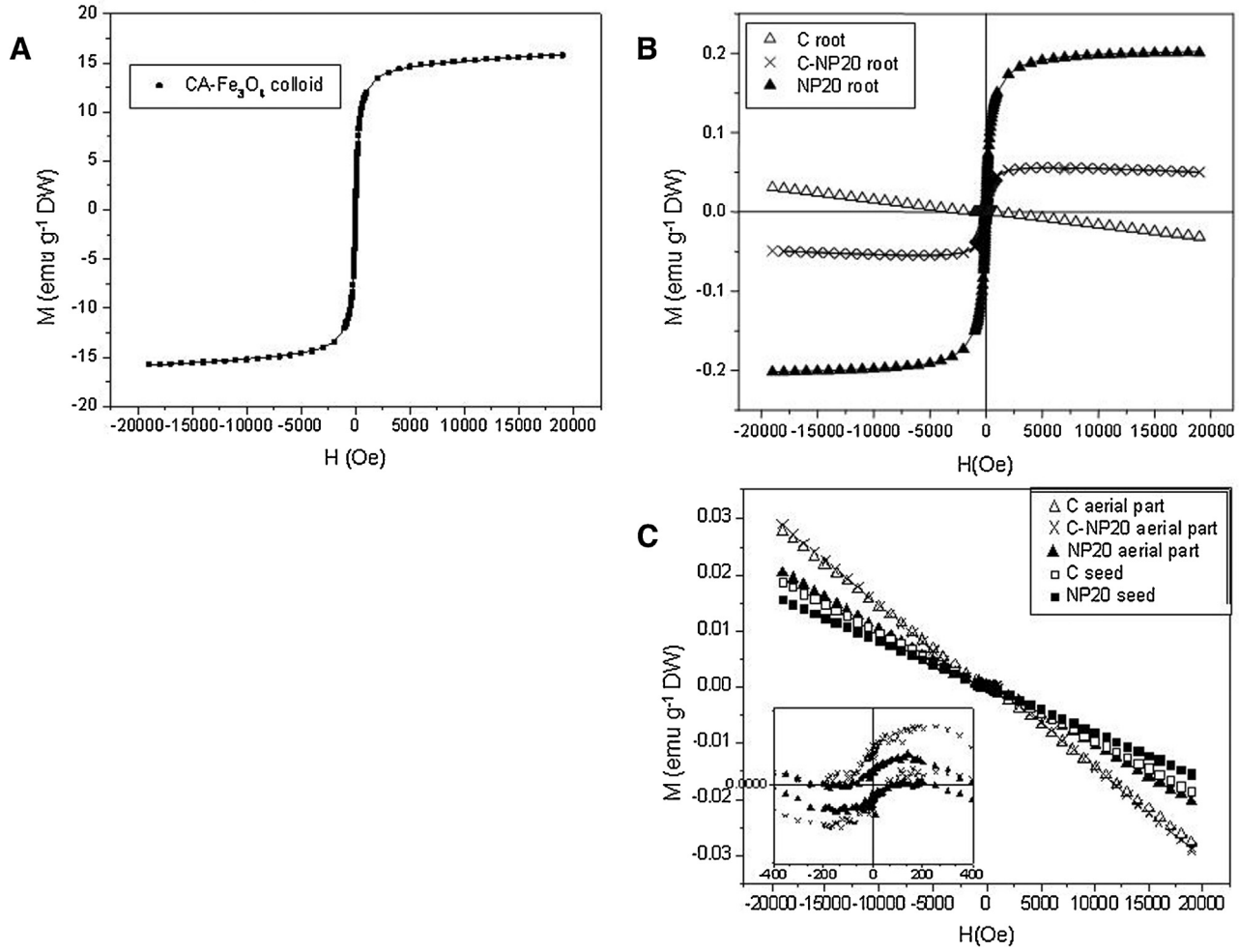

Fig. 4. Selected magnetization results by vibrating sample magnetometer (VSM) of wheat roots, seeds and aerial part samples. Panel (A) shows the VSM loops of CA-Fe_3O_4 colloid. Panel (B) shows magnetization loops *vs.* applied field H of C, C-NP20, NP20 roots samples. Panel (C) shows the VSM loops of C, NP20 seeds samples and C, C-NP20, NP20 aerial part samples. In all Figures, M (emu g^{-1} DW) and H (Oe) represent magnetization and applied magnetic field, respectively. C, NP20, C-NP20 mean control plants, plants treated with 20 mg L^{-1} Fe_3O_4 nanoparticles from germination, plants treated with 20 mg L^{-1} Fe_3O_4 nanoparticles after germination, respectively.

exposed to the colloid along with germination than after germination.

3.5. Nanoparticles localization

Fig. 5 shows TEM cross sections images of the plant tissues after treatment with 20 mg L^{-1} Fe_3O_4 NPs from germination (NP20) or after germination (C-NP20). Fe_3O_4 NPs, visualized as dark dots, were found in roots exposed to the NPs after germination (Fig. 5B–D) or from germination (Fig. 5E–G) and they were localized in the outer surface of the root epidermal cell wall (Fig. 5D) and in the intercellular space (Fig. 5E) of the root cells. The TEM measured size of these dark dots was 10.53 ± 1.64 ($n = 20$), identical to the size of Fe_3O_4 NPs. Such dark dots (*i.e.*, particles) were not observed in control roots (Fig. 5A), neither in seeds nor in the aerial part exposed to the nanoparticles (data not shown).

3.6. Study of oxidative stress and antioxidants parameters

3.6.1. Hydrogen peroxide and superoxide anion accumulation

Hydrogen peroxide production was visualized by staining roots or leaves with 3, 3′-diaminobenzidine (DAB). Both, roots and leaves treated with magnetite nanoparticles revealed no significant differences in H_2O_2 production compared to controls on any condition tested. The specificity of the reaction was confirmed by infiltrating the roots or leaves with ascorbate prior to staining with DAB (data not shown).

In accordance, magnetite nanoparticles treatment did not produce significant differences in $O_2^{\bullet -}$ accumulation (measured by NBT staining) in roots or leaves in any condition evaluated (data not shown).

3.6.2. Antioxidant enzymes activity

The activity of the main H_2O_2-detoxifying enzymes (CAT, APOX, GPOX, SOD) was measured to evaluate the antioxidant machinery of wheat plants subjected to NP treatment. In general terms, NP treatment (at germination or after germination) produced an increase in the antioxidant enzyme activities. However, different levels of response were observed according to the treatment applied and the NP concentration used. CAT activity was duplicated in roots and the aerial parts of wheat plants grown from germination in 5 and 15 mg L^{-1} magnetite (NP5, NP15, $p < 0.05$). In plants treated with magnetite nanoparticle after germination, the enzyme activity raised twice with 15 and 20 mg L^{-1} magnetite (C-NP15, $p < 0.01$; C-NP20, $p < 0.05$) only in the aerial part.

In roots, APOX activity increased 39%, 45%, 77% and 96% when plants were treated with 5, 10, 15 and 20 mg L^{-1} magnetite from germination (NP5 and NP10, $p < 0.05$; NP15 and NP20, $p < 0.01$, respectively) and augmented 55%, 76%, 59% in plants treated with 10, 15, 20 mg L^{-1} magnetite after germination (C-NP10, $p < 0.05$;

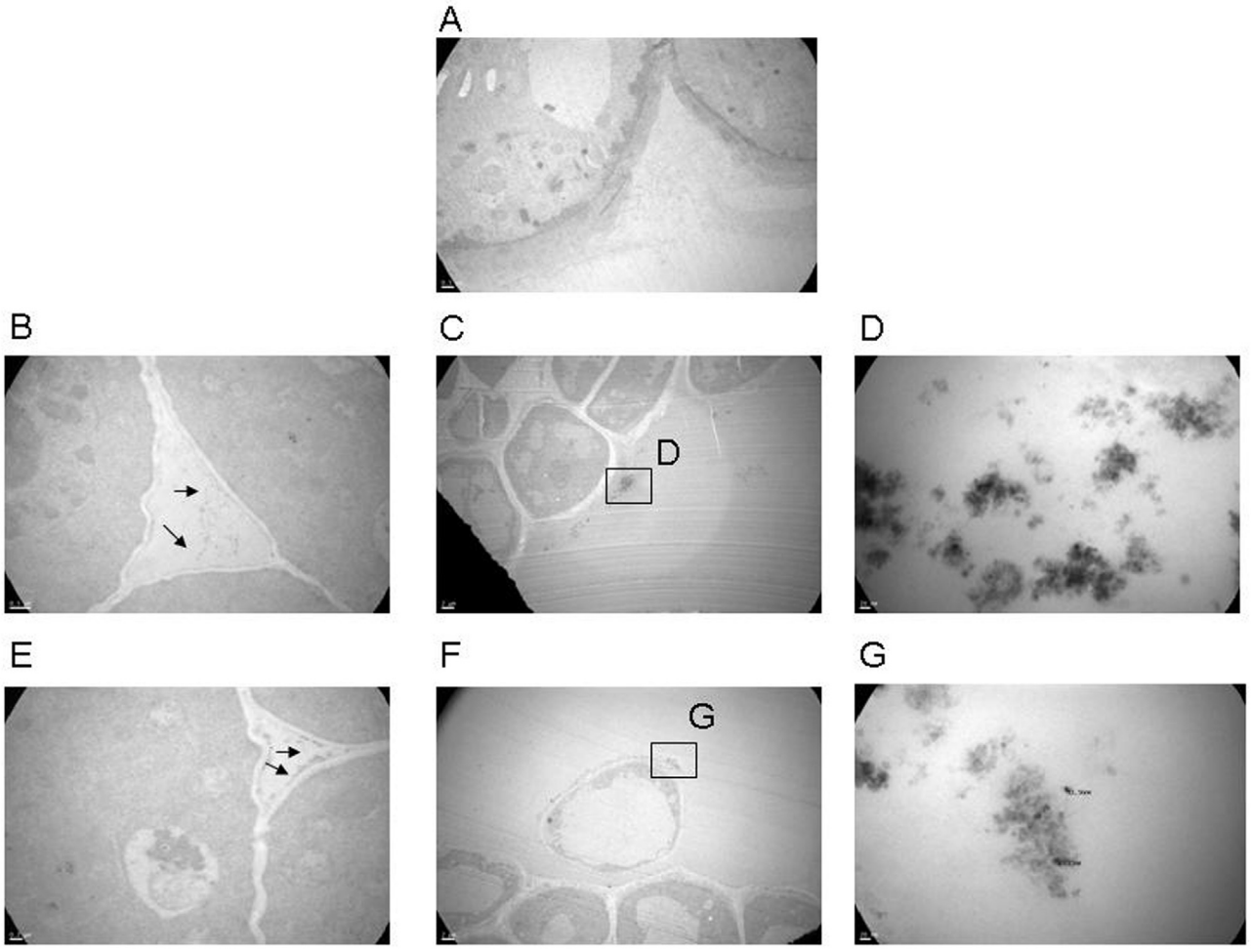

Fig. 5. Transmission-electron microscope (TEM) scans of the roots of *Triticum aestivum* L. exposed to 20 mg L^{-1} Fe_3O_4 nanoparticles: (A) control (12,000×), (B) C-NP20 (20,000×), (C) C-NP20 (3000×), (D) Magnification from the area inside the rectangle in panel C (250,000×), (E) NP20 (30,000×), (F) NP20 (3000×), (G) Magnification from the area inside the rectangle in panel F (250,000×). Arrows indicate the presence of nanoparticles.

C-NP15, $p < 0.01$; C-NP20, $p < 0.05$). APOX activity in the aerial part increased 65% in NP5 treatment ($p < 0.05$), and between 40% to 60% in wheat plants treated with the NPs after germination (C-NP5, C-NP10, C-NP15, C-NP20; $p < 0.05$).

GPOX activity significantly increased in roots exposed to almost all NP concentrations. When NP were supplied from germination, GPOX activity augmented 18 and 10 times with 5 and 10 mg L^{-1} F_3O_4 NPs, respectively (NP5 and NP10, $p < 0.001$), whereas 15 and 20 mg L^{-1} F_3O_4 NPs tripled or doubled the enzyme activity respect to its control (NP15, $p < 0.001$; NP20, $p < 0.01$). In the aerial part, there was an increase of 80%, 62% and 19% in GPOX activity in wheat plants treated with 10, 15, 20 mg L^{-1} NP from germination, respectively (NP10, NP15, $p < 0.01$; NP20, $p < 0.05$). When wheat plants were exposed to the NPs after germination, GPOX activity increased 39% with 5 mg L^{-1} F_3O_4 NPs (C-NP5, $p < 0.05$), while 10 and 20 mg L^{-1} F_3O_4 NPs (C-NP10, $p < 0.01$; C-NP20, $p < 0.01$) duplicated its value and C-NP15 treatment triplicated the enzyme activity in roots ($p < 0.001$). It was observed an increment of GPOX activity of 30% with 5 mg L^{-1} NP(C-NP5, $p < 0.05$) in the aerial part of wheat plants.

SOD activity, which is a major source of H_2O_2 derived from superoxide anion in plant cells, doubled its value with 15 mg L^{-1} NP (NP15, $p < 0.01$) in roots and the aerial parts, 20 mg L^{-1} NP rose its activity by 40% and 35% (NP20, $p < 0.05$), while no differences were observed using the other NP concentrations tested. In the aerial parts of plants exposed to the nanoparticles after germination, it was observed an activity rise of 33%, 53%, 19% and 22% with 5, 10, 15, 20 mg L^{-1} NP, respectively (C-NP5, $p < 0.05$; C-NP10, $p < 0.01$; C-NP15, $p < 0.05$; C-NP20, $p < 0.05$). In roots, 10 mg L^{-1} NP doubled the enzyme activity (C-NP10, $p < 0.01$), while 20 mg L^{-1} NP augmented it 42% (C-NP20, $p < 0.05$; Table 2 and Table 3).

3.6.3. Evidence of oxidative damage and cell death: TBARS content, electrolyte leakage and Evans blue staining

TBARS content, electrolyte leakage and Evans blue were measured to evaluate the extent of oxidative damage and cell death under magnetite exposure.

As shown in Fig. 6A and B, there was no evidence of lipid peroxidation in none of the treatments evaluated in both roots and aerial parts of wheat plants. Surprisingly, some treatments (NP5, NP10, NP15) diminished TBARS content below control values.

Regarding ion leakage, no symptoms of damage were observed in roots and the aerial parts of wheat plants in the conditions tested, except for a decrease in this parameter in the aerial part using 10 mg L^{-1} and 15 mg L^{-1} magnetite nanoparticle from germination (NP10 and NP15, $p < 0.05$; Fig. 6C).

No evidence of cell death estimated by Evans blue staining was detected in roots or aerial parts of wheat plants treated with F_3O_4 NPs from or after germination at any of the nanoparticle concentrations tested (Fig. 6E,F).

Table 2
Effect of Fe_3O_4 nanoparticles on antioxidant enzymes activities in roots and aerial part of wheat (*Triticum aestivum* L.) plants exposed to the nanoparticle from germination.

		C	NP5	NP10	NP15	NP20
CAT	Root	0.52 ± 0.15	0.98 ± 0.22*	0.48 ± 0.02	1.23 ± 0.22*	0.66 ± 0.12
(pmol g^{-1} FW s^{-1})	Aerial part	1.29 ± 0.16	2.15 ± 0.33*	1.42 ± 0.08	2.76 ± 0.40*	1.99 ± 0.28*
APOX	Root	19.21 ± 1.1	26.7 ± 3.80*	27.85 ± 0.25*	34.01 ± 3.30**	37.70 ± 2.20**
(nmol g^{-1} FW s^{-1})	Aerial part	7.54 ± 0.90	12.48 ± 1.79*	5.99 ± 0.12	5.35 ± 0.41	9.20 ± 2.36
GPOX	Root	3.96 ± 0.02	70.46 ± 0.18***	39.63 ± 0.20***	13.02 ± 0.01***	7.11 ± 0.07**
(nmol g^{-1} FW)	Aerial part	18.54 ± 0.18	15.97 ± 0.05	33.55 ± 0.18**	30.09 ± 0.10**	22.04 ± 0.07*
SOD	Root	11.07 ± 0.45	12.71 ± 0.29	9.41 ± 0.44	23.31 ±0.65**	15.42 ± 0.37*
(U g^{-1} FW)	Aerial part	11.31 ± 0.52	13.29 ± 0.73	11.14 ± 1.40	21.37 ± 0.82**	15.24 ± 0.31*

Plants exposed to 5 (NP5), 10 (NP10), 15 (NP15), 20 (NP20) mg L^{-1} Fe_3O_4 nanoparticles from germination. Data are the mean ± S.E. of two independent experiments, with five replicates for each treatment. Asterisks indicate significant differences (*, $p < 0.05$; **, $p < 0.01$; ***, $p < 0.001$) according to Tukey's multiple range test. Enzymatic activities were assayed as described in Materials and Methods. One unit of CAT is the amount of the enzyme that oxidized 1 pmol of H_2O_2 min^{-1} under the assay conditions. One unit of APOX forms 1 nmol of oxidized ascorbate min^{-1} under the assay conditions. One unit of GPOX is the amount of the enzyme that reduced 1 nmol of H_2O_2 min^{-1} under the assay conditions. One unit of SOD is the amount of the enzyme that inhibits the reduction of NBT by 50% under the assay conditions.

4. Discussion

In the field of agriculture, the use of nanomaterials is relatively new and requires further study (Khot et al., 2012). NPs have begun to be used in agriculture with potential applications in numerous areas, for example, in order to increase the effectiveness of herbicides and pesticides which can be administered at lower doses (Rico et al., 2011), as fertilizer to increase crop productivity (Dimkpa and Bindraban, 2016), for crop protection and production, as well as detection of pathogens and pesticide/herbicide residues (Khot et al., 2012; Mohammadinejad et al., 2016). In this sense, Dikshit et al. (2013) reported that new formulations could include nanoparticles in order to improve the bacterial growth and consequently the inoculant quality.

Due to the possible role of NPs as tools of controlled release of agrochemicals, bioinoculants and nutrients in the soil, it is essential to study their toxicity in plants.

In wheat seeds, neither superparamagnetic signal nor augmented Fe content was detected, indicating that magnetite NPs could not enter into the seed probably due to the selective permeability of the seed coat or the size of Fe_3O_4 NPs, thereafter germination was not affected (Fig. 2). The role of seed coat in protecting the embryo from harmful external factors has been reported by Wierzbicka and Obidzin'ska, (1998). After germination, root tip accumulation of nutrients is important because the tip contains stem cells (*i.e.*, undifferentiated cells able to divide into many tissue types) such as root meristem and columella initials that are needed for root growth and production of the root cap.

The presence of black dots in TEM images of the root cells, an increase in the total Fe content respect to the control and the magnetization detected in roots demonstrated an evident uptake of magnetite (Fe_3O_4) NPs by wheat roots. It is noteworthy that Fe accumulation was dependent on the time of exposure to the nanoparticles and the plant stage since NP20 treatment increased twenty times the Fe content while wheat plants exposed to the NPs after germination, C-NP20 treatment, quintupled the Fe content of control roots. At germination stage, seeds use nutrients in high amounts to start germination and growth, so elevated levels of magnetite were uptaked by wheat plants at that stage. However, that high amount of NPs was not harmful to wheat plants.

NPs have been reported as either being able or unable to be taken up and translocated by plants. Not surprisingly, several groups have shown that the accumulation and translocation of metal-based NPs in plants is also species-specific (Ma et al., 2015).

As an example, Zhu et al. (2008) did not detect magnetism in the tissues of lima bean plants grown in a Fe_3O_4 NP suspension, but they observed that these NPs entered and accumulated in pumpkin (*Cucurbita maxima*) plants, whereas Wang et al. (2011) did not observe any uptake of 25 nm Fe_3O_4 NPs in pumpkin (*Cucurbita mixta* cv. white cushaw) plants suggesting that the uptake and translocation of NPs is, at least, partially dependent on plant species. Superparamagnetic iron oxide NPs were absorbed and transported in soybean plants causing an increase in chlorophyll levels, with no trace of toxicity (Ghafariyan et al., 2013). By the way, neither Doshi et al. (2008) nor Wang et al. (2011) observed uptake of aluminum NPs by California red beans or magnetite NPs by *Cucurbita mixta* plants, respectively. Although, many studies have demonstrated NPs translocation in plants, the mechanisms remain unclear (Ma et al., 2015).

Once inside the roots, NPs could be translocated to the aerial part. However, Fe_3O_4 NPs were not transported to shoots in wheat plants, since no superparamagnetic behaviour was detected in the aerial part of the plants (Fig. 4C), total Fe content in the shoots of plants treated with Fe_3O_4 NPs was similar to controls (Table 1), and TEM images did not showed black dots in the aerial part (data not shown). The aggregation of nanoparticles in root apoplast may complicate their passage through plasmodesmata, as well as the translocation through the vascular system, possibly due to their size. However, silver NPs entered root hair cells and then vascular tissue of *Arabidopsis* plants, and once in the vascular tissues, they

Table 3
Effect of Fe_3O_4 nanoparticles on antioxidant enzymes activities in roots and aerial part of wheat (*Triticum aestivum* L.) plants exposed to the nanoparticle after germination.

		C	C-NP5	C-NP10	C-NP15	C-NP20
CAT	Root	0.50 ± 0.10	0.45 ± 0.02	0.40 ± 0.09	0.38 ± 0.08	0.54 ± 0.12
(pmol g^{-1} FW s^{-1})	Aerial part	1.24 ± 0.06	1.01 ± 0.09	1.15 ± 0.23	3.20 ± 0.95**	2.78 ± 1.02*
APOX	Root	19.81 ± 2.89	24.97 ± 4.80	30.64 ± 1.79*	34.83 ± 5.41**	31.61 ± 5.46*
(nmol g^{-1} FW s^{-1})	Aerial part	7.60 ± 0.53	12.13 ± 0.50*	10.83 ± 1.40*	10.53 ± 0.57*	11.50 ± 2.51*
GPOX	Root	4.15 ± 0.20	5.76 ± 0.18*	9.35 ± 0.20**	13.95 ± 0.10***	8.22 ± 0.10**
(nmol g^{-1} FW)	Aerial part	18.58 ± 0.05	24.24 ± 0.20*	20.87 ± 0.10	15.91 ± 0.78	18.77 ± 0.09
SOD	Root	11.05 ± 0.25	9.67 ± 0.92	24.54 ± 0.34**	12.72 ±0.95	15.66 ± 0.28*
(U g^{-1} FW)	Aerial part	11.94 ± 0.42	15.95 ± 0.33*	18.28 ± 0.66**	14.23 ± 0.22*	14.61 ± 0.28*

Plants exposed to 5 (C-NP5), 10 (C-NP10), 15 (C-NP15), 20 (C-NP20) mg L^{-1} Fe_3O_4 nanoparticles after germination. Data are the mean ± S.E. of two independent experiments, with five replicates for each treatment. Asterisks indicate significant differences (*, $p < 0.05$; **, $p < 0.01$; ***, $p < 0.001$) according to Tukey's multiple range test. Enzymatic activities were assayed as described in Materials and Methods. One unit of CAT is the amount of the enzyme that oxidized 1 pmol of H_2O_2 min^{-1} under the assay conditions. One unit of APOX forms 1 nmol of oxidized ascorbate min^{-1} under the assay conditions. One unit of GPOX is the amount of the enzyme that reduced 1 nmol of H_2O_2 min^{-1} under the assay conditions. One unit of SOD is the amount of the enzyme that inhibits the reduction of NBT by 50% under the assay conditions.

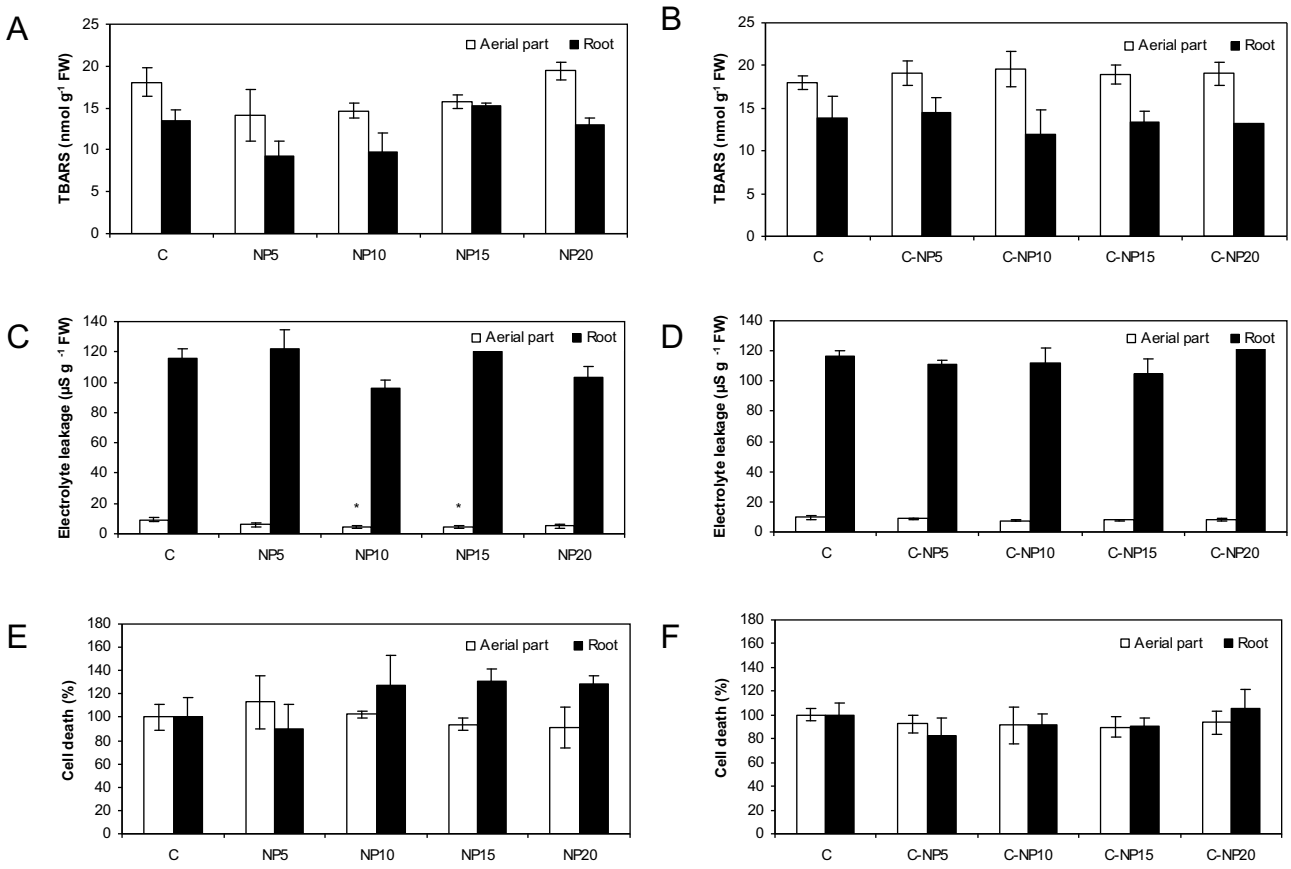

Fig. 6. Oxidative damage and cell death measured as TBARS content (A,B), electrolyte leakage (C,D) and Evans blue staining (E,F) in wheat (*Triticum aestivum* L.) plants exposed to 5, 10, 15, 20 mg L^{-1} Fe_3O_4 nanoparticles from germination (NP5, NP10, NP15, NP20) or after germination (C-NP5, C-NP10, C-NP15, C-NP20). Values are the mean ± SE of three different experiments with six replicated measurements. Asterisks indicate significant differences (*, $p < 0.05$) according to Tukey's multiple range test.

could be transported throughout the whole plant (Geisler-Lee et al., 2014). Carbon-coated magnetic NPs can be absorbed by sunflower, tomato or wheat plant root systems and spread using the vascular system to reach the whole plant in the first 24 h of exposure to a suspension of carbon-coated magnetic NPs, and in the case of wheat, they accumulated inside leaf trichomes (Cifuentes et al., 2010).

Nevertheless, it should be taken into account that modifications of the growth media, for example with the addition of surfactants, could also alter the aggregation of NPs, thus allowing their movement to other parts of the plants (European Commission Scientific Committee on Emerging and Newly Identified Health Risks, 2006). In this context, modifications of NPs surface could modify the cell uptake and translocation (Zhang et al., 2002). Therefore, further investigations in relation to the uptake, translocation, and accumulation of NPs in different plant species grown under diverse growing conditions are required in order to understand their mechanisms of action and/or toxicity.

6.1. Phytotoxicity evaluation

The percentage of germination of *Triticum aestivum* L. seeds was not affected by magnetite-nanoparticle treatment, in accordance with the results reported by de la Rosa et al. (2011) in *Parkinsonia florida* (blue palo verde), *Prosopis juliflora-velutina* (velvet mesquite) and *Salsola tragus* (tumbleweed) treated with ZnO NPs. In *Chinese mung bean* seeds, the effect of Fe_3O_4 NPs depended on the NPs concentration; while 10 mg L^{-1} NPs inhibited germination, 20 mg L^{-1} promoted it (Ren et al., 2011). Meanwhile, Arora et al. (2012) observed that gold nanoparticles stimulated germination of *B. juncea* seeds, but the root length of *Arabidopsis* seedlings grown on nutrient agar plates containing 100 mg L^{-1} gold were reduced by 75%. Oxidized gold was subsequently found in roots and shoots of these plants, but gold NPs (reduced gold) were only observed in the root tissues (Taylor et al., 2014).

Growth retardation and the decrease in chlorophyll content are general symptoms of phytotoxicity. However, these symptoms were not observed in wheat plants under Fe_3O_4 NPs treatments. Even more, NP15, NP20 and C-NP15 treatments enhanced root growth, which would be beneficial to increase nutrient uptake by the plant. In addition, C-NP5 also caused an increment in the aerial part length (Figs. 2 and 3), showing that this type of NPs could be useful for several purposes, not only because they did not reduce plant growth but even could favour it. In our experimental system, the lack of toxicity observed could be due to the chemical composition and surface properties of citric acid coated-Fe_3O_4 nanoparticles rather than its size, as suggested by Ghafariyan et al. (2013), who reported that nanomaterial phytotoxicity was related to its chemical composition, size, surface properties, and ionization of the surface.

Several reports have published contrasting results using NPs to test different plant health parameters. An increase in chlorophyll content was reported in *Asparagus* treated with silver NPs, in *Brassica juncea* treated with Au NPs, and in Chinese mung bean treated with Fe_3O_4 NPs (An et al., 2008; Arora et al., 2012; Ren et al., 2011), whereas Fe_3O_4 NPs nutrient suspension could accelerate the growth of sprout (Ren et al., 2011). Lin and Xing (2007) observed that the influence of NPs on seed germination and root growth varied according to the type of NPs (multi-walled carbon nanotube, aluminum, alumina, zinc, and zinc oxide) and plant species (radish,

rape, ryegrass, lettuce, corn, and cucumber). In this sense, silver and copper NPs inhibited the growth of *Cucurbita pepo* (Musante and White, 2010), silver NPs affected the growth of phytoplankton (Miao et al., 2007), whereas root elongation of *Parkinsonia florida*, *Salsola tragus*, and *Prosopis juliflora-velutina* was inhibited by ZnO NPs (de la Rosa et al., 2011).

6.2. Oxidative stress and cell death evaluation

Reactive oxygen species (ROS) play essential roles in growth, development and interactions with the environment in plants and therefore they are produced in significant amounts during photosynthesis and respiration.

The main ROS produced in plants are hydrogen peroxide (H_2O_2) and superoxide radical $O_2^{\bullet -}$. Meanwhile, the redox homeostasis is maintained by mechanisms which control synthesis and degradation (Halliwell, 2006) of radical species. Uncontrolled increase in ROS production triggers complex detoxification mechanisms that involve both enzymatic (superoxide dismutase, catalase and peroxidases, mainly) and non-enzymatic systems (glutathione, ascorbate, *etc*), which are able to prevent uncontrolled oxidation of biological molecules like proteins or lipids (Gill and Tuteja, 2010). The imbalance between ROS production and detoxification in organisms leads to what is known as oxidative stress. Besides, ROS generation is known to be a primary factor that results in cell membrane damage through lipid peroxidation, leading to ion leakage and potential cell death.

Nanoparticles are often more reactive than its bulk material, mainly due to the increase of their surface area/volume ratio (Iravani, 2011), and so far there is no consensus whether NPs produce more oxidative burst than its bulk counterpart. In this sense, the effect of iron oxides NPs on the oxidative/antioxidative response of the plant was also assayed. Magnetite nanoparticles neither produced ROS accumulation nor membrane damage, evaluated by lipid peroxidation and electrolyte leakage both in roots and aerial part of wheat plants at any tested condition (Figs. 4–6). Cell death was not observed in plants exposed to nanoparticles (Fig. 6E,F). In addition, wheat plants responded to NP treatment by increasing the enzymatic antioxidant defence system (CAT, GPOX, APOX, SOD) thus preventing the potential oxidative damage in wheat tissues. Although magnetite NPs were not translocated to the aerial part, an augmented antioxidant enzymes activity was observed in these tissues. It has been suggested that ROS or NO can travel from roots to shoots as ROS waves and can exert an effect in distant tissues from the place of formation (Gilroy et al., 2014; Mittler et al., 2011; Steinhorst and Kudla, 2013). Moreover they could be acting as signalling molecules and thus inducing the antioxidant enzyme response even in distant tissues. Similarly, Wang et al. (2011) reported an increased in SOD and CAT activity in roots and shoots but magnetite NPs were not found in ryegrass or pumpkin leaves. Additionally, the authors observed that magnetite NPs, coated by polyvinylpyrrolidone (PVP) with a diameter of 25 nm, produced more oxidative stress than bulk particles.

Citric acid coated-Fe_3O_4 nanoparticles seemed not to be toxic in wheat plants in the studied conditions. Similar results were observed in soybean plants (unpublished data).

Although the exact mechanisms of plant defence against nanotoxicity are unclear, several relevant studies have been recently published (Ma et al., 2015).

Some authors have reported the effect of iron NPs on oxidative damage production, but different results were obtained dependent on the assay conditions. In Chinese mung beans, the presence or not of lipid peroxidation was related to the size of the NP used (Ren et al., 2011). However, the authors observed a decrease in catalase and peroxidase enzyme activities, regardless the concentration or size of the NP tested, whereas SOD activity was inhibited in a NP concentration and size dependent manner. In plants of ryegrass (*Lolium perenne* L.) and squash (*Cucurbita mixta* cv. White cushaw), the increase of catalase activity caused by magnetite NPs was not enough to avoid the lipid damage (Wang et al., 2011). In a similar way, Zhao et al. (2012) observed H_2O_2 accumulation in maize shoots exposed to CeO_2 nanoparticles, despite the increase in catalase and ascorbate peroxidase activities. However, they did not detect changes in the levels of lipid peroxidation, or in the electrolytes release. Using gold NPs, Arora et al. (2012) observed a reduction in malondialdehyde content in *Brassica juncea* plants. Besides, these authors found no significant differences in H_2O_2 content using 10 ppm of gold NPs but H_2O_2 content increased by 29% with 100 ppm. In this context, the balance or imbalance between the ROS production and detoxification may depend on the type, size and concentration of NPs, the exposure time and the plant species used for the study. For example, CAT activity in wheat roots was significantly elevated upon treatment with 500 mg/kg CuO NPs, whereas inhibition of CAT activity was observed at 500 mg/kg ZnO NPs treatment, suggesting that other detoxification pathways may be important for ROS scavenging (Dimkpa et al., 2012).

In order to fully characterize the mechanisms involved in the antioxidant defence system induced by metal-based NPs, additional investigations should be necessary. The pattern of isoenzymes should be useful in order to determine if not only the total enzyme activity but different isoenzymes were modified in response to NPs in wheat roots and shoots. As it was described by Soares et al. (2016), Ni did not change the SOD isoenzyme pattern in *Solanum nigrum* L, but they observed an increased in all SOD isoenzymes and in the total SOD activity in Ni exposed plants. Besides, Boaretto et al. (2014) reported that sugarcane drought-tolerant cultivar (IACSP 94-2094) responded differently to water stress compared to a commercial cultivar in Brazil (IACSP 95-5000), and CAT shift in isoenzymes pattern in the tolerant cultivar might have contributed to this response.

7. Conclusion

In summary, we demonstrated that a significant amount of Fe_3O_4 NPs suspended in a liquid medium can be taken up by wheat plants after seed germination. Particles tended to accumulate in the roots but they were not translocated throughout the whole plant since neither superparamagnetic signals nor TEM images of Fe_3O_4 nanoparticles were detected in wheat leaves. Interestingly, these NPs were not toxic for wheat plants as they did not change the cell death percentage, nor the electrolyte release or TBARS content, neither the H_2O_2 and $O_2^{\bullet -}$ accumulation. Even more, the antioxidant enzymes activity increased significantly, showing a favourable response to prevent oxidative damage.

These preliminary results suggest that Fe_3O_4 NPs could be used as agrochemicals releasers. Nevertheless, a deeper insight of the interaction of Fe_3O_4 NPs with soil rizhosphere and the influence of essential nutrients on NPs uptake and translocation in wheat and other plants species are needed in order to know their possible transportation through the food chain with a consequent impact on human health.

Acknowledgements

This work was supported by the University of Buenos Aires (Project UBACYT 20020100100295) and CONICET (PIP 0097). Nanoparticle synthesis and magnetic analysis were performed at the Instituto de Física de La Plata (IFLP)/Universidad Nacional de La Plata (UNLP), Argentina under grant PIP 0720 of CONICET and X556 of UNLP.

Iannone MF, Groppa MD, Benavides MP and Fernández van Raap MB are researchers of the Consejo Nacional de Investigaciones Científicas y Técnicas (CONICET) and de Sousa ME is a fellow of CONICET.

References

An, J., Zhang, M., Wang, S., Tang, J., 2008. Physical, chemical and microbiological changes in stored green asparagus spears as affected by coating of silver nanoparticles-PVP. LWT—Food Sci. Technol. 41, 1100–1107.

Arora, S., Sharma, P., Kumar, S., Nayan, R., Khanna, P.K., Zaidi, M.G.H., 2012. Gold–nanoparticle induced enhancement in growth and seed yield of Brassica juncea. Plant Growth Regul. 66, 303–310.

Arruda, S.C.C., Silva, A.L.D., Galazzi, R.M., Azevedo, R.A., Arruda, M.A.Z., 2015. Nanoparticles applied to plant science: a review. Talanta 131, 693–705. doi:http://dx.doi.org/10.1016/j.talanta.2014.08.050.

Baker, C.J., Mock, N.M., 1994. An improved method for monitoring cell death in cell suspension and leaf disc assays using Evans blue. Plant Cell Tissue Organ Cult. 39, 7–12.

Becana, M., Aparicio-Tejo, P., Irigoyen, J.J., Sánchez-Díaz, M., 1986. Some enzymes of hydrogen peroxide metabolism in leaves and root nodules of Medicago sativa. Plant Physiol. 82, 1169–1171.

Boaretto, L.F., Carvalho, G., Borgo, L., Creste, S., Landell, M.G.A., Mazzafera, P., Azevedo, R.A., 2014. Water stress reveals differential antioxidant responses of tolerant and non-tolerant sugarcane genotypes. Plant Physiol. Biochem. 74, 165–175.

Bolwell, G.P., Davies, D.R., Gerrish, C., Auh, C.-K., Murphy, T.M., 1998. Comparative biochemistry of the oxidative burst produced by rose and French bean cells reveals two distinct mechanisms. Plant Physiol. 116, 1379–1385.

Chance, B., Sies, H., Boveris, A., 1979. Hydroperoxide metabolism in mammalian organs. Physiol. Rev. 59, 527–605.

Chichiriccò, G., Poma, A., 2015. Penetration and toxicity of nanomaterials in higher plants. Nanomaterials 5, 851–873;. doi:http://dx.doi.org/10.3390/nano5020851.

Cifuentes, Z., Custardoy, L., de la Fuente, J.M., Marquina, C., Ibarra, M.R., Rubiales, D., Pérez-de-Luque, A., 2010. Absorption and translocation to the aerial part of magnetic carbon–coated nanoparticles through the root of different crop plants. J. Nanobiotechnol. 8, 26.

de Sousa, M.E., Fernandez van Raap, M.B., Rivas, P.C., Mendoza Zélis, P., Girardin, P., Pasquevich, G.A., Alessandrini, J.L., Muraca, D., Sánchez, F.H., 2013. Stability and relaxation mechanisms of citric acid coated magnetite nanoparticles for magnetic hyperthermia. J. Phys. Chem. C 117, 5436–5445.

de la Rosa, G., Lopez–Moreno, M.L., Hernandez–Viezcas, J., Montes, M.O., Peralta—Videa, J.R., 2011. Toxicity and biotransformation of ZnO nanoparticles in the desert plants Prosopis juliflora-velutina, Salsola tragus and Parkinsonia florida. Int. J. Nanotechnol. 8, 492–506.

Dikshit, A., Shukla, S.K., Mishra, R.K., 2013. Exploring Nanomaterials with PGPR in Current Agricultural Scenario. Lambert Academic Publising, Saarbrucken Germany, pp. 51.

Dimkpa, C.O., Bindraban, P., 2016. Fortification of micronutrients for efficient agronomic production: a review. Agron. Sustain. Dev. 36 (1), 1–26. doi:http://dx.doi.org/10.1007/s13593-015-0346-6.

Dimkpa, C., McLean, J., Latta, D., Manango'n, E., Britt, D., Johnson, W., Boyanov, M., Anderson, A., 2012. CuO and ZnO nanoparticles: phytotoxicity, metal speciation, and induction of oxidative stress in sand grown wheat. J. Nanopart. Res. 14, 1–15.

Doshi, R., Braida, W., Christodoulatos, C., Wazne, M., O'Connor, G., 2008. Nano–aluminum: transport through sand columns and environmental effects on plants and soil communities. Environ. Res. 106, 296–303.

Eggenberger, K., Birtalan, E., Schröder, T., Bräse, S., Nick, P., 2009. Passage of Trojan peptoids into plant cells. Chembiochem 10, 2504–2512.

Modified opinion (after public consultation) on the appropriateness of existing methodologies to assess the potential risks associated with engineered and adventitious products of nanotechnologies. pp. 13–14.

Fleischer, A., O'Neill, M.A., Ehwald, R., 1999. The pore size of non–graminaceous plant cell walls is rapidly decreased by borate ester cross–linking of the pectic polysaccharide rhamnogalacturonan II. Plant Physiol. 121, 829–838.

Frahry, G., Schopfer, P., 1998. Inhibition of $O_2^{\cdot-}$- reducing activity of horseradish peroxidase by diphenyleneiodonium. Phytochemistry 48, 223–227.

Gao, L.Z., Zhuang, J., Nie, L., Zhang, J.B., Zhang, Y., Gu, N., Wang, T.H., Feng, J., Yang, D. L., Perrett, S., Yan, X., 2007. Intrinsic peroxidase–like activity of ferromagnetic nanoparticles. Nat. Nanotechnol. 2, 577.

Geisler-Lee, J., Brooks, M., Gerfen, J.R., Wang, Q., Fotis, C., Sparer, A., Ma, X., Berg, R.H., Geisler, M., 2014. Reproductive toxicity and life history study of silver nanoparticle effect, uptake and transport in Arabidopsis thaliana. Nanomaterials 4, 301–318.

Ghafariyan, M.H., Malakouti, M.J., Dadpour, M.R., Stroeve, P., Mahmoudi, M., 2013. Effects of magnetite nanoparticles on soybean chlorophyll. Environ. Sci. Technol. 47, 10645–10652.

Ghalamboran, M.R., Ramsden, J.J., 2010. Viability of Bradyrhizobium japonicum on soybean seeds enhanced by magnetite nanoparticles during desiccation. World Acad. Sci. Eng. Technol. 4, 188–193.

Ghalamboran, M.R., Ramsden, J.J., Ansari, F., 2009. Growth rate enhancement of Bradyrhizobium japonicum due to magnetite nanoparticles. J. Bionanosci. 3, 1–6.

Gill, S.S., Tuteja, N., 2010. Reactive oxygen species and antioxidant machinery in abiotic stress tolerance in crop plants. Plant Physiol. Biochem. 48, 909–930.

Gilroy, S., Suzuki, N., Miller, G., Choi, W.G., Toyota, M., Devireddy, A.R., Mittler, R., 2014. A tidal wave of signals: calcium and ROS at the forefront of rapid systemic signaling. Trends Plant Sci. 19 (10), 623–630. doi:http://dx.doi.org/10.1016/j.tplants.2014.06.013.

Gojon, A., Nacry, P., Davidian, J.C., 2009. Root uptake regulation: a central process for NPS homeostasis in plants. Curr. Opin. Plant Biol. 12, 328–338.

Halliwell, B., 2006. Reactive species and antioxidants. Redox biology is a fundamental theme of aerobic life. Plant Physiol. 141, 312–322.

Heath, R.L., Packer, L., 1968. Photoperoxidation in isolated chloroplasts: I. Kinetics and stoichiometry of fatty acid peroxidation. Arch. Biochem. Biophys. 125, 189–198.

Hoagland, D.R., Arnon, D.I., 1950. The water–culture method for growing plants without soil. Circular, University of California, College of Agriculture, Agricultural Experiment Station 347, 42.

Hossain, Z., Mustafa, G., Komatsu, S., 2015. Plant responses to nanoparticle stress. Int. J. Mol. Sci. 16, 26644–26653. doi:http://dx.doi.org/10.3390/ijms161125980.

Iravani, S., 2011. Green synthesis of metal nanoparticles using plants. Green Chem. 13, 2638–2650.

Khot, L.R., Sankaran, S., Maja, J.M., Ehsani, R., Schuster, E.W., 2012. Applications of nanomaterials in agricultural production and crop protection: a review. Crop Prot. 35, 64–70.

Kohler, N., Sun, C., Wang, J., Zhang, M., 2005. Methotrexate–modified superparamagnetic nanoparticles and their intracellular uptake into human cancer cells. Langmuir 21, 8858–8864.

Lin, D., Xing, B., 2007. Phytotoxicity of nanoparticles: inhibition of seed germination and root growth. Environ. Pollut. 150, 243–250.

Lin, D., Xing, B., 2008. Root uptake and phytotoxicity of ZnO nanoparticles. Environ. Sci. Technol. 42, 5580–5585.

Liu, J.F., Zhao, Z.S., Jiang, G.B., 2008. Coating Fe_3O_4 magnetic nanoparticles with humic acid for high efficient removal of heavy metals in water. Environ. Sci. Technol. 42, 6949–6954.

Ma, X., Geisler-Lee, J., Deng, J., Kolmakov, A., 2010. Interactions between engineered nanoparticles (ENPs) and plants phytotoxicity, uptake and accumulation. Sci. Total Environ. 408, 3053–3061.

Ma, C., White, J.C., Dhankher, O.P., Xing, B., 2015. Metal-based nanotoxicity and detoxification pathways in higher plants. Environ. Sci. Technol. 49, 7109–7122. doi:http://dx.doi.org/10.1021/acs.est.5b00685.

Maehly, A.C., Chance, B., 1954. The assay of catalase and peroxidasa. Methods Biochem. Anal. 1, 357–424.

Mahmoudi, M., Sant, S., Wang, B., Laurent, S., Sen, T., 2011. Superparamagnetic iron oxide nanoparticles (SPIONs) development, surface modification and applications in chemotherapy. Adv. Drug Deliv. Rev. 63, 24–46.

Miao, A.J., Quigg, A., Schwehr, K., Xu, C., Santschi, P., 2007. Engineered silver nanoparticles (ESNs) in coastal marine environments: bioavailability and toxic effects to the phytoplankton Thalassiosira weissflogii. 2nd International Conference on the Environmental Effects of Nanoparticles and Nanomaterials, 24–25th September, London UK.

Miralles, P., Church, T.L., Harris, A.T., 2012. Toxicity, uptake, and translocation of engineered nanomaterials in vascular plants. Environ. Sci. Technol. 46, 9224–9239.

Mittler, R., Vanderauwera, S., Suzuki, N., Miller, G., Tognetti, V.B., Vandepoele, K., Gollery, M., Shulaev, V., Van Breusegem, F., 2011. ROS signaling: the new wave? Trends Plant Sci. 16 (6), 300–309. doi:http://dx.doi.org/10.1016/j.tplants.2011.03.007.

Miwa, K., Tanaka, M., Kamiya, T., Fujiwara, T., 2010. Molecular mechanisms of boron transport in plants: involvement of Arabidopsis NIP5;1 and NIP6;1. Adv. Exp. Med. Biol. 679, 83–96.

Mohammadinejad, R., Karimi, S., Iravani, S., Varma, R.S., 2016. Plant-derived nanostructures: types and applications. Green Chem. 18, 20–52. doi:http://dx.doi.org/10.1039/c5gc01403d.

Morneau, A., Pillai, V., Nigam, S., Winnik, F.M., Ziolo, R.F., 1999. Analysis of ferrofluids by capillary electrophoresis. Colloids Surf. A: Physicochem. Eng. Asp. 154, 295–301.

Musante, C., White, J.C., 2010. Toxicity of silver and copper to Cucurbita pepo: differential effects of nano and bulk-size particles. Environ. Toxicol. doi:http://dx.doi.org/10.1002/tox.20667.

Nakano, Y., Asada, K., 1981. Hydrogen peroxide is scavenged by ascorbate-specific peroxidase in spinach choroplast. Plant Cell Physiol. 22, 867–880.

Ren, H.X., Liu, L., Liu, C., He, S.-H., Huang, J., Li, J.-L., Zhang, Y., Huang, X.-J., Gu, N., 2011. Physiological investigation of magnetic iron oxide nanoparticles towards Chinese mung bean. J. Biomed. Nanotechnol. 7, 677–684.

Rico, C.M., Majumdar, S., Duarte-Gardea, M., Peralta-Videa, J.R., Gardea-Torresdey, J. L., 2011. Interaction of nanoparticles with edible plants and their possible implications in the food chain. J. Agric. Food Chem. 59, 3485–3498.

Sahoo, Y., Goodarzi, A., Swihart, M.T., Ohulchanskyy, T.Y., Kaur, N., Furlani, E.P., Prasad, P.N., 2005. Aqueous ferrofluid of magnetite nanoparticles: fluorescence labeling and magnetophoretic control. J. Phys. Chem. 109, 3879–3885.

Shipley, H.J., Engates, K.E., Guettner, A.M., 2011. Study of iron oxide nanoparticles in soil for remediation of arsenic. J. Nanopart. Res. 13, 2387–2397.

Shou, H., Bordallo, P., Fan, J.-B., Yeakley, J.M., Bibikova, M., Sheen, J., Wang, K., 2004. Expression of an active tobacco mitogen-activated protein kinase enhances freezing tolerance in transgenic maize. Proc. Natl. Acad. Sci. U. S. A. 101, 3298–3303.

Soares, C., de Sousa, A., Pinto, A., Azenha, M., Teixeira, J., Azevedo, R.A., Fidalgo, F., 2016. Effect of 24-epibrassinolide on ROS content, antioxidant system, lipid peroxidation and Ni uptake in Solanum nigrum L. under Ni stress. Environ. Exp. Bot. 122, 115–125.

Steinhorst, L., Kudla, J., 2013. Calcium and reactive oxygen species rule the waves of signaling. Plant Physiol. 163, 471–485.

Taylor, A.F., Rylott, E.L., Anderson, C.W.N., Bruce, N.C., 2014. Investigating the toxicity, uptake nanoparticle formation and genetic response of plants to gold. PLoS One 9 (4), e93793. doi:http://dx.doi.org/10.1371/journal.pone.0093793.

Thordal-Christensen, H., Zhang, Z., Wei, Y., Collinge, D.B., 1997. Subcellular localization of H_2O_2 in plants, H_2O_2 accumulation in papillaeand hypersensitive response during the barley-powdery mildew interaction. Plant J. 11, 1187–1194.

Wang, H., Kou, X., Pei, Z., Xiao, J.Q., Shan, X., Xing, B., 2011. Physiological effects of magnetite (Fe_3O_4) nanoparticles on perennial ryegrass (Lolium perenne L.) and pumpkin (Cucurbita mixta) plants. Nanotoxicology 5, 30–42.

Wang, Z., Xie, X., Zhao, J., Liu, X., Feng, W., White, J.C., Xing, B., 2012. Xylem–and phloem–based transport of CuO nanoparticles in maize (Zea mays L.). Environ. Sci. Technol. 46, 4434–4441.

Wierzbicka, M., Obidzin'ska, J., 1998. The effect of lead on seed imbibition and germination in different plant species. Plant Sci. 137, 155–171.

Wintermans, J.F., de Mots, A., 1965. Spectrophotometric characteristics of chlorophylls a and b and their pheophytins in ethanol. Biochim. Biophys. Acta 109, 448–453.

Yantasee, W., Warner, C.L., Sangvanich, T., Addleman, R.S., Carter, T.G., Wiacek, R.J., Fryxell, G.E., Timchalk, C., Warner, M.G., 2007. Removal of heavy metals from aqueous systems with thiol functionalized superparamagnetic nanoparticles. Environ. Sci. Technol. 41, 5114–5119.

Zhang, Y., Kohler, N., Zhang, M., 2002. Surface modification of superparamagnetic magnetite nanoparticles and their intracellular uptake. Biomaterials 23, 1553–1561.

Zhao, L., Peng, B., Hernandez-Viezcas, J.A., Rico, C., Sun, Y., Peralta-Videa, J.R., Tang, X., Niu, G., Jin, L., Varela-Ramirez, A., Zhang, J.Y., Gardea-Torresdey, J.L., 2012. Stress response and tolerance of Zea mays to CeO_2 nanoparticles: cross talk among H_2O_2, heat shock protein, and lipid peroxidation. ACS Nano 6, 9615–9622. doi:http://dx.doi.org/10.1021/nn302975u.

Zhu, H., Han, J., Xiao, J.Q., Jin, Y., 2008. Uptake, translocation, and accumulation of manufactured iron oxide nanoparticles by pumpkin plants. J. Environ. Monit. 10, 713–717.

Zins, D., Cabuil, V., Massart, R., 1999. New aqueous magnetic fluids. J. Mol. Liq. 83, 217–232.